PHYSICAL REVIEW D **96,** 111502(R) (2017)

Correlations of the energy-momentum tensor via gradient flow in SU(3) Yang-Mills theory at finite temperature

Masakiyo Kitazawa,[1,2,*] Takumi Iritani,[3] Masayuki Asakawa,[1] and Tetsuo Hatsuda[3,4]

[1]*Department of Physics, Osaka University, Toyonaka, Osaka 560-0043, Japan*
[2]*J-PARC Branch, KEK Theory Center, Institute of Particle and Nuclear Studies, KEK, 203-1, Shirakata, Tokai, Ibaraki 319-1106, Japan*
[3]*Theoretical Research Division, Nishina Center, RIKEN, Wako 351-0198, Japan*
[4]*iTHEMS Program and iTHES Research Group, RIKEN, Wako 351-0198, Japan*

(Received 8 August 2017; published 22 December 2017)

Euclidean two-point correlators of the energy-momentum tensor (EMT) in SU(3) gauge theory on the lattice are studied on the basis of the Yang-Mills gradient flow. The entropy density and the specific heat obtained from the two-point correlators are shown to be in good agreement with those from the one-point functions of EMT. These results constitute a first step toward the first principle simulations of the transport coefficients with the gradient flow.

DOI: 10.1103/PhysRevD.96.111502

Various thermal and transport properties of quantum field theories are encoded in the correlations of energy-momentum tensor (EMT) at finite temperature (T). In particular, fluctuation and transport properties of hot QCD (quantum chromodynamics) matter at finite T have attracted a lot of attention in relation to the phenomenological studies on relativistic heavy-ion collisions [1,2].

Although the nonperturbative investigations of the EMT at finite T using lattice QCD simulations have been very difficult owing to the lack of translational and rotational symmetry [3,4], a novel method to construct the EMT on the lattice [5] on the basis of the gradient flow [6–8] was recently proposed and was successfully applied to the equation of states in pure gauge theory [9–11].[1] This study shows that the thermodynamical observables such as the energy density and pressure extracted from the expectation values of the EMT (the one-point functions) agree extremely well with previous high-precision results using the integral method [14–16]. Also, the statistics required in the new method is substantially smaller than that in the previous method. The method is now extended to full QCD simulations at finite T [17,18].

In the present paper, we report our exploratory studies to extend the previous results of the one-point functions to the two-point EMT correlators in SU(3) lattice gauge theory [19]. The advantages of such extension are threefold. First of all, the method allows direct access to the specific heat c_V and entropy density s from the EMT correlations. Second, one could explicitly check the conservation law of EMT obtained by the gradient flow. Third, the method will open the new door to the study of important transport coefficients such as the shear and bulk viscosities [20–24]. We will focus on the first two aspects in this paper.

Let us here summarize the properties of the correlators of the EMT, $\mathcal{T}_{\mu\nu}(x)$, in the Euclidean and continuum space-time, where $x_{\mu=1,2,3,4} = (\vec{x}, \tau)$ with $0 \le \tau < 1/T$. We define a dimensionless temporal correlator of $\mathcal{T}_{\mu\nu}(x)$ at finite T and at finite volume V as

$$C_{\mu\nu;\rho\sigma}(\tau) \equiv \frac{1}{T^5}\int_V d^3x \langle \delta\mathcal{T}_{\mu\nu}(x)\delta\mathcal{T}_{\rho\sigma}(0)\rangle, \tag{1}$$

where $\langle\cdot\rangle$ denotes the thermal average and we defined $\delta\mathcal{T}_{\mu\nu}(x) \equiv \mathcal{T}_{\mu\nu}(x) - \langle\mathcal{T}_{\mu\nu}(x)\rangle$ [5]. Note that $C_{\mu\nu;\rho\sigma}(\tau)$ contains only connected contribution. Owing to the conservation of the EMT in the Euclidean space-time ($\partial_\mu \mathcal{T}_{\mu\nu} = 0$), we have $\frac{d}{d\tau}\bar{\mathcal{T}}_{4\nu} = 0$ with $\bar{\mathcal{T}}_{\mu\nu} \equiv \int_V d^3x \mathcal{T}_{\mu\nu}(x)$. For $\tau \neq 0$, this leads to

$$\frac{d}{d\tau} C_{4\nu;\rho\sigma}(\tau) = 0. \tag{2}$$

Since the energy density of the system is represented as $\varepsilon = -\langle\bar{\mathcal{T}}_{44}\rangle/V$, the specific heat per unit volume c_V is given by [2]

$$\frac{c_V}{T^3} = \frac{1}{T^3}\frac{d\varepsilon}{dT} = \frac{\langle(\delta\bar{\mathcal{T}}_{44})^2\rangle}{VT^5} = C_{44;44}(\tau), \tag{3}$$

where Eq. (2) is used in the last equality. Note that τ can be taken anywhere in the range $0 < \tau < 1/T$ owing to the EMT conservation.

Similarly, from the thermodynamic relation for entropy density $s = dp/dT = (1/V)d\langle\bar{\mathcal{T}}_{11}\rangle/dT$ [25], one obtains

$$\frac{s}{T^3} = \frac{1}{T^3}\frac{dp}{dT} = \frac{\langle\delta\bar{\mathcal{T}}_{44}\delta\bar{\mathcal{T}}_{11}\rangle}{VT^5} = -C_{44;11}(\tau). \tag{4}$$

Again, τ can be taken arbitrarily in $0 < \tau < 1/T$.

*kitazawa@phys.sci.osaka-u.ac.jp

[1]For other recent progress in the construction of the EMT on the lattice, see Refs. [4,12,13].

Finally, the momentum fluctuation is related to the enthalpy density h [12,26],

$$\frac{h}{T^4} = \frac{\langle (\delta \bar{T}_{41})^2 \rangle}{VT^5} = -C_{41;41}(\tau). \tag{5}$$

At zero chemical potential, $h = \varepsilon + p = sT$.

The gradient flow for Yang-Mills gauge field is defined by the differential equation with respect to the hypothetical 5th coordinate t [7]

$$\frac{dA_\mu(t,x)}{dt} = -g_0^2 \frac{\delta S_{\rm YM}(t)}{\delta A_\mu(t,x)} = D_\nu G_{\nu\mu}(t,x), \tag{6}$$

with the Yang-Mills action $S_{\rm YM}(t)$ and the field strength $G_{\mu\nu}(t,x)$ composed of the transformed field $A_\mu(t,x)$. The flow time t has a dimension of inverse mass squared. The initial condition at $t = 0$ is taken for the field in the conventional gauge theory; $A_\mu(0,x) = A_\mu(x)$. The gradient flow for positive t acts as the smearing of the gauge field. Since the mean square radius of the flow in D dimensional Euclidean space is $\sqrt{2Dt}$, this length is employed as the smearing radius of the gradient flow in Ref. [7]. On the other hand, when the smearing along one direction is concerned, the smearing radius is given by $\sqrt{2t}$ irrespective of the space dimension.

The renormalized EMT operator is then obtained as

$$\mathcal{T}^{\rm R}_{\mu\nu}(x) = \lim_{t\to 0} \mathcal{T}_{\mu\nu}(t,x), \tag{7}$$

$$\mathcal{T}_{\mu\nu}(t,x) = \frac{U_{\mu\nu}(t,x)}{\alpha_U(t)} + \frac{\delta_{\mu\nu}}{4\alpha_E(t)}[E(t,x) - \langle E(t,x)\rangle_0], \tag{8}$$

where the dimension-four gauge-invariant operators on the right-hand side are given by [5]

$$E(t,x) = \frac{1}{4} G^a_{\mu\nu}(t,x) G^a_{\mu\nu}(t,x), \tag{9}$$

$$U_{\mu\nu}(t,x) = G^a_{\mu\rho}(t,x) G^a_{\nu\rho}(t,x) - \delta_{\mu\nu} E(t,x), \tag{10}$$

while $\langle E(t,x)\rangle_0$ in Eq. (8) is the vacuum expectation value of $E(t,x)$, so that $\langle \mathcal{T}^{\rm R}_{\mu\nu}(x)\rangle$ vanishes in the vacuum. The coefficients $\alpha_U(t)$ and $\alpha_E(t)$ have been calculated perturbatively in Ref. [5] for small t: Their explicit forms in the $\overline{\rm MS}$ scheme are given in Ref. [11].

Although Eqs. (7) and (8) are exact in the continuum spacetime, special care is required in lattice gauge theory with finite lattice spacing a: The flow time should satisfy $2\sqrt{2t} \gtrsim a$ to suppress the lattice discretization effects. It has been shown for the thermal average of the EMT that there exists indeed a range of t for sufficiently small a, so that the lattice data allow reliable extrapolation to $t = 0$ to obtain ε and p [9–11]. Moreover, it is shown in Ref. [11] that results agree with those obtained by the integral method [16] within a few percent level. This shows that the use of perturbative coefficients in Eq. (8) is enough to define the EMT within this accuracy as long as the proper double limit ($t \to 0$ after $a \to 0$) is taken.

To analyze the two-point EMT correlations with Eq. (8), we have an extra condition that the distance between the two smeared operators τ in temporal direction is well separated (with the temporal periodicity) to avoid their overlap. Then the necessary conditions read

$$a \lesssim 2\sqrt{2t} \lesssim \tau \le \tau_m, \tag{11}$$

with $\tau_m \equiv 1/(2T)$, or equivalently, in terms of the dimensionless quantities, $1/N_\tau \lesssim 2\sqrt{2tT^2} \lesssim \tau T \le 1/2$, with $N_\tau = (aT)^{-1}$ being the temporal lattice size.

In our numerical studies, we consider SU(3) Yang-Mills theory on four-dimensional Euclidean lattice and employ the Wilson gauge action under the periodic boundary condition. Gauge configurations are generated by the same procedure as in Ref. [11], but each measurement is separated by 50 sweeps. Statistical errors are estimated by the jackknife method with 100 jackknife samples. On the right-hand side of the flow equation Eq. (6), the Wilson gauge action is used for $S_{\rm YM}(t)$, while the operators in Eqs. (9) and (10) are constructed from $G^a_{\mu\nu}(t,x)$ defined by the clover-type representation.

We study two cases above the deconfinement transition, $T/T_{\rm c} = 1.68$ and 2.24, with three different lattice volumes $N_s^3 \times N_\tau$ with a fixed aspect ratio $N_s/N_\tau = 4$. The values of $\beta = 6/g_0^2$ corresponding to each set of $T/T_{\rm c}$ and N_τ are obtained from Refs. [11,27]. The resultant simulation parameters are summarized in Table I.

Shown in Fig. 1 are the τ dependences of $C_{44;44}(\tau)$, $C_{44;11}(\tau)$, and $C_{41;41}(\tau)$ for $T/T_{\rm c} = 1.68$ (upper panels) and

TABLE I. Simulation parameters on the lattice: N_s, N_τ, $\beta = 6/g_0^2$, and $N_{\rm conf}$ are spatial lattice size, temporal lattice size, the bare coupling constant, and the total number of gauge configurations, respectively.

$T/T_{\rm c} = 1.68$			
N_s	N_τ	β	$N_{\rm conf}$
96	24	7.265	200 000
64	16	6.941	180 000
48	12	6.719	180 000
$T/T_{\rm c} = 2.24$			
N_s	N_τ	β	$N_{\rm conf}$
96	24	7.500	200 000
64	16	7.170	180 000
48	12	6.943	180 000

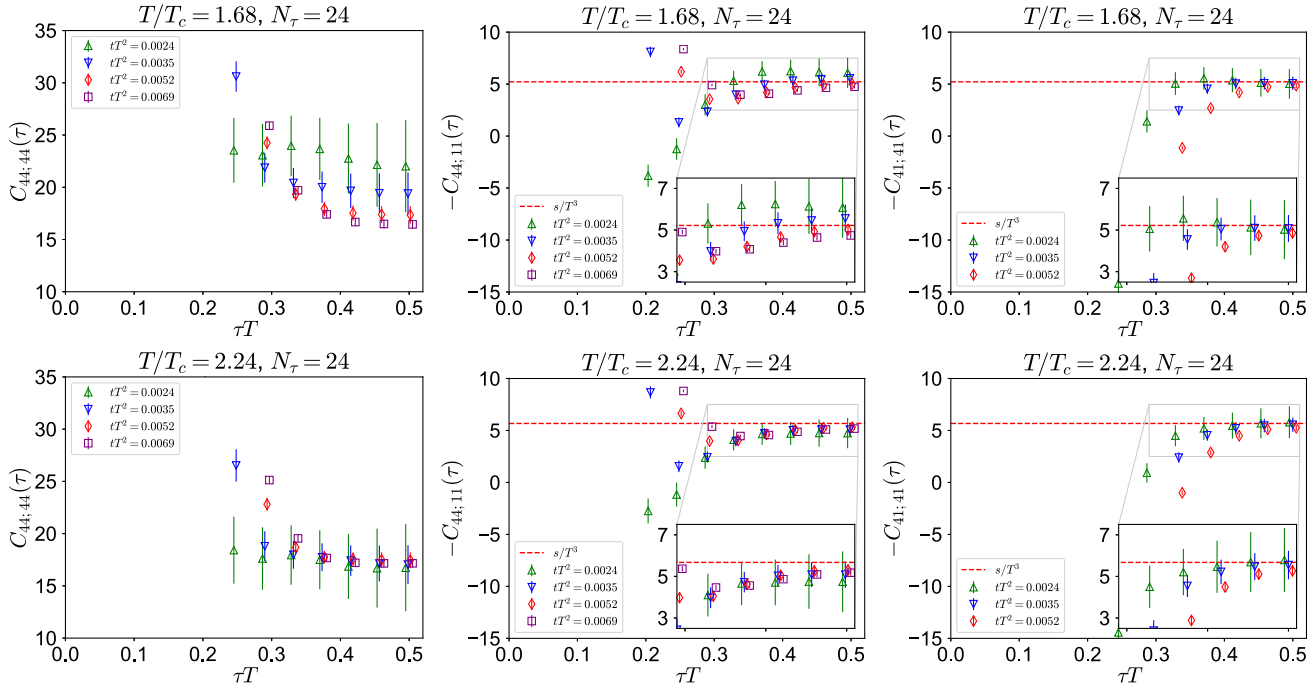

FIG. 1. Correlators $C_{44;44}(\tau)$ (left), $C_{44;11}(\tau)$ (middle), and $C_{41,41}(\tau)$ (right) for several values of flow time t for $N_\tau = 24$. The red dashed lines show $s/T^3 = (\varepsilon + p)/T^4$ obtained from the one-point function of the EMT with the same gauge configurations.

$T/T_c = 2.24$ (lower panels) for $N_\tau = 24$ with typical values of tT^2 between the upper and lower bounds in Eq. (11). From the overall behavior of the lattice data in these figures, one finds two key features: (i) As t decreases, the data start to show the plateau structure for $\tau T \gtrsim 0.3$. (ii) As t decreases, the statistical errors become larger. The feature (i) is a signature of the EMT conservation Eq. (2) for large τ, where the smeared EMT operators do not overlap

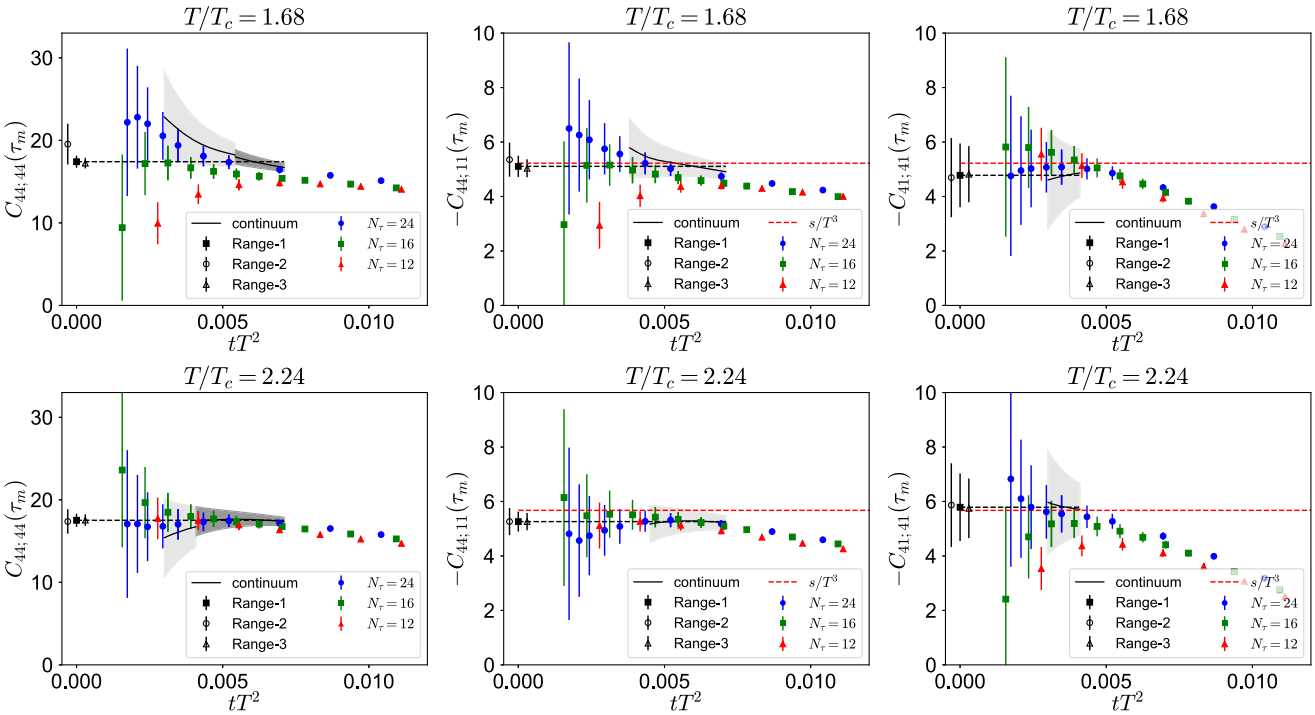

FIG. 2. t dependences of the midpoint correlators $C_{44,44}(\tau_m)$ (left), $C_{44,11}(\tau_m)$ (middle), and $C_{41,41}(\tau_m)$ (right) for $T/T_c = 1.68$ and 2.24. The black lines show the results of continuum extrapolation, where the dark and light error bands represent the results with three and two lattice spacings, respectively (see text).

with each other. The feature (ii) is due to the fact that the gauge fields are rough (smooth) for small (large) t.

Shown by the red dashed lines in Fig. 1 together with $C_{44;11}(\tau)$ and $C_{41;41}(\tau)$ are $s/T^3 = (\varepsilon + p)/T^4$ obtained by the one-point function of EMT ($\langle \bar{\mathcal{T}}_{44} \rangle$ and $\langle \bar{\mathcal{T}}_{11} \rangle$) using the method in Ref. [11] with the same configurations. This agreement of the results of s/T^3 between the one-point function and the two-point functions, as it should be for Eqs. (4) and (5), at large τ and small t indicates an internal consistency of the present method.

To take the continuum limit $a \to 0$ followed by an extrapolation $t \to 0$, we show, in Fig. 2, the t dependence of the correlators for different lattice spacings, $a = 1/(N_\tau T)$. Here we choose the maximum possible separation, $\tau = \tau_m$, to minimize the overlap of the EMT operators. The continuum extrapolation is carried out by using the data at $N_\tau = 12$, 16, and 24 for each $t \in [t_{\min}, t_{\max}]$ with an ansatz $C_{\mu\nu;\rho\sigma}(\tau_m)|_{\rm lat} = C_{\mu\nu;\rho\sigma}(\tau_m)|_{\rm cont} + O(a^2)$ expected from perturbation theory. Here we select the data to be used for the continuum extrapolation as follows. First of all, we consider the data only in the region $2\sqrt{2t} < \tau_m/2$ to avoid oversmearing. This is a conservative condition which is more stringent than Eq. (11) by a factor of two. (Note that we chose $\tau = \tau_m$.) Second, we impose a condition that the conservation law, $C_{4\nu;\rho\sigma}(\tau_m)/C_{4\nu;\rho\sigma}(\tau_m - a) = 1$, is satisfied within 5% accuracy. These two requirements not only determine the window $t_{\min} < t < t_{\max}$ but also select the data points to be used for $N_\tau = 12$, 16, and 24 given t. Accordingly, the continuum extrapolation is taken either by using data for $N_\tau = 12$, 16, and 24 or by those for $N_\tau = 16$ and 24. This procedure excludes the small t region where large lattice discretization errors arise, as well as the large t region where the systematic errors from the overlap of EMT operators and the contribution of higher dimensional operators other than Eqs. (9) and (10) are not negligible [11].

The results of the continuum extrapolation are shown by the black lines with the error represented by the gray band in Fig. 2. The continuum extrapolated results with three (two) lattice spacings are shown by dark (light) error band. At the level of error bars in the present exploratory study, we do not have enough resolution to reliably extract the $O(t)$ contribution in $C_{\mu\nu;\rho\sigma}(\tau_m)$ [11], so that we take the $t \to 0$ extrapolation by a constant fit in the interval $[t_{\min}, t_{\max}]$, which is called Range-1. The final results after the double extrapolation ($t \to 0$ after $a \to 0$) are shown by the filled squares in Fig. 2. To estimate the systematic errors from this constant fit, we choose the Range-2 (the first half of Range-1) and Range-3 (the latter half of Range-1); the results are shown by open circles and open triangles, respectively. The red dashed lines in the middle and right panels in Fig. 2 are s/T^3 obtained from the one-point function of EMT.

TABLE II. Values of s/T^3 obtained from Eqs. (4) and (5) together with those obtained from the one-point function of EMT. The ideal gas limit for massless gluons is also shown for comparison. The first (second) parenthesis shows statistical (systematic) error. The systematic error for the one-point function originates from the 1% uncertainty of $\Lambda_{\overline{\rm MS}}$ [11].

s/T^3				
T/T_c	$C_{44;11}(\tau_m)$	$C_{41;41}(\tau_m)$	$\langle \mathcal{T}^{\rm R}_{\mu\nu} \rangle$	ideal gas
1.68	$5.11(39)(^{+24}_{-7})$	$4.78(1.17)(^{+4}_{-9})$	5.222(10)(24)	7.02
2.24	$5.26(37)(^{+0}_{-0})$	$5.79(1.24)(^{+7}_{-4})$	5.675(10)(24)	7.02

TABLE III. Values of c_V/T^3 obtained by Eq. (3) as well as those obtained directly from the differential method [28] and those calculated indirectly from $\varepsilon(T)$ in the integral method [16]. The ideal gas limit for massless gluons is also shown for comparison. The error bars are estimated in the same way as s/T^3 in Table II. The symbol $*$ ($**$) indicates that the numbers are for $T/T_c = 1.5(2.0)$. The error bars of c_V/T^3 in the column Ref. [16] would be a few % level.

c_V/T^3				
T/T_c	$C_{44;44}(\tau_m)$	Ref. [28]	Ref. [16]	ideal gas
1.68	$17.4(7)(^{+2.1}_{-0.2})$	$22.8(7)^*$	17.7	21.06
2.24	$17.5(8)(^{+0}_{-0.1})$	$17.9(7)^{**}$	18.2	21.06

Shown in Table II are the numerical results of s/T^3 obtained in the present analysis of EMT correlators. Within the statistical and systematic error bars, the results of the two different correlators agree with each other, and they agree to the results of the one-point function of EMT. Also the central value of s/T^3 in our analysis increases as T and also much less than the ideal gas value, which captures the essential feature expected from strongly interacting gluon plasma above T_c.

Shown in Table III are the numerical results of c_V/T^3 obtained in the present analysis of EMT correlators. Our results agree quantitatively with the numbers extracted from the recent high-precision study of the energy density in the integral method [16] and qualitatively with the numbers obtained in the differential method [28]. Our specific heat is about 20% smaller than the ideal gas value, which also indicates the strong coupling feature of the system.

In summary, we have investigated the two-point EMT correlators in SU(3) Yang-Mills theory at finite temperature ($T/T_c = 2.24$ and 1.68) using the method of gradient flow with the flow time t. The correlators $C_{4\nu;\rho\sigma}(\tau)$ approach constant values for sufficiently large τ and small t. This is an indication that the conservation of the EMT is realized in the gradient flow as long as the two EMT operators do not

have overlap with each other. By taking the double limit ($t \to 0$ after $a \to 0$) using the data for $N_\tau = 12$, 16, and 24, we found that the entropy density (s) obtained from the two-point EMT correlators ($C_{44;11}(\tau_m)$ and $C_{41;41}(\tau_m)$) reproduces the high precision result previously obtained from the one-point function. Also, we found that the specific heat (c_V) can be determined in 5-10% accuracy from the two-point EMT correlator ($C_{44;44}(\tau_m)$). Now that we have confirmed that thermodynamical quantities are obtained accurately with two-point EMT correlators with the gradient flow, it is within reach to investigate transport coefficients with two-point EMT correlations as well.

Although we focused on SU(3) Yang-Mills theory in this study, the same analysis can be also performed in full QCD [17,18]. A preliminary study along this line is reported in Ref. [29,30].

ACKNOWLEDGMENTS

The authors thank E. Itou and H. Suzuki for discussions in the early stage. Numerical simulation was carried out on IBM System Blue Gene Solution at KEK under its Large-Scale Simulation Program (Nos. 13/14-20, 14/15-08, 15/16-15, 16/17-07). This work was supported by JSPS KAKENHI Grant Nos. JP17K05442 and 25287066. T. H. was partially supported by the RIKEN iTHES Project and iTHEMS Program. T. H. is grateful to the Aspen Center for Physics, supported by NSF Grant No. PHY1607611, where part of this research was done.

[1] T. Hirano, P. Huovinen, K. Murase, and Y. Nara, Integrated dynamical approach to relativistic heavy ion collisions, Prog. Part. Nucl. Phys. **70**, 108 (2013).
[2] M. Asakawa and M. Kitazawa, Fluctuations of conserved charges in relativistic heavy ion collisions: An introduction, Prog. Part. Nucl. Phys. **90**, 299 (2016).
[3] S. Caracciolo, G. Curci, P. Menotti, and A. Pelissetto, The energy momentum tensor for lattice gauge theories, Ann. Phys. (N.Y.) **197**, 119 (1990).
[4] H. Suzuki, Energy–momentum tensor on the lattice: Recent developments, *Proc. Sci.*, LATTICE2016 (2017) 002, [arXiv:1612.00210], and references therein.
[5] H. Suzuki, Energy-momentum tensor from the Yang-Mills gradient flow, Prog. Theor. Exp. Phys. **13**, 083B03 (2013); Erratum, Prog. Theor. Exp. Phys. **2015**, 079201 (2015).
[6] R. Narayanan and H. Neuberger, Infinite N phase transitions in continuum Wilson loop operators, J. High Energy Phys. 03 (2006) 064.
[7] M. Lüscher, Properties and uses of the Wilson flow in lattice QCD, J. High Energy Phys. 08 (2010) 071.
[8] M. Lüscher and P. Weisz, Perturbative analysis of the gradient flow in non-abelian gauge theories, J. High Energy Phys. 02 (2011) 051.
[9] M. Asakawa, T. Hatsuda, E. Itou, M. Kitazawa, and H. Suzuki (FlowQCD Collaboration), Thermodynamics of SU(3) gauge theory from gradient flow on the lattice, Phys. Rev. D **90**, 011501 (2014); Erratum, Phys. Rev. D **92**, 059902 (2015).
[10] N. Kamata and S. Sasaki, Numerical study of tree-level improved lattice gradient flows in pure Yang-Mills theory, Phys. Rev. D **95**, 054501 (2017).
[11] M. Kitazawa, T. Iritani, M. Asakawa, T. Hatsuda, and H. Suzuki, Equation of state for SU(3) gauge theory via the energy-momentum tensor under gradient flow, Phys. Rev. D **94**, 114512 (2016).
[12] L. Giusti and H. B. Meyer, Thermal Momentum Distribution from Path Integrals with Shifted Boundary Conditions, Phys. Rev. Lett. **106**, 131601 (2011); Implications of Poincare symmetry for thermal field theories in finite-volume, J. High Energy Phys. 01 (2013) 140.
[13] L. Giusti and M. Pepe, Energy-momentum tensor on the lattice: Nonperturbative renormalization in Yang-Mills theory, Phys. Rev. D **91**, 114504 (2015).
[14] G. Boyd, J. Engels, F. Karsch, E. Laermann, C. Legeland, M. Lutgemeier, and B. Petersson, Thermodynamics of SU(3) lattice gauge theory, Nucl. Phys. **B469**, 419 (1996).
[15] M. Okamoto *et al.* (*CP*-PACS Collaboration), Equation of state for pure SU(3) gauge theory with renormalization group improved action, Phys. Rev. D **60**, 094510 (1999).
[16] S. Borsanyi, G. Endrodi, Z. Fodor, S. D. Katz, and K. K. Szabo, Precision SU(3) lattice thermodynamics for a large temperature range, J. High Energy Phys. 07 (2012) 056.
[17] H. Makino and H. Suzuki, Lattice energy–momentum tensor from the Yang–Mills gradient flow–inclusion of fermion fields, Prog. Theor. Exp. Phys. **2014**, 63B02 (2014); **2015**, 079202 (2015).
[18] Y. Taniguchi, S. Ejiri, R. Iwami, K. Kanaya, M. Kitazawa, H. Suzuki, T. Umeda, and N. Wakabayashi, Exploring $N_f = 2 + 1$ QCD thermodynamics from gradient flow, Phys. Rev. D **96**, 014509 (2017);
[19] Preliminary results of this study is reported in M. Kitazawa *et al.* Measurement of thermodynamics using gradient flow, *Proc. Sci.*, LATTICE2014 (2014) 022, [arXiv:1412.4508].
[20] F. Karsch and H. W. Wyld, Thermal Green's functions and transport coefficients on the lattice, Phys. Rev. D **35**, 2518 (1987).
[21] A. Nakamura and S. Sakai, Transport Coefficients of Gluon Plasma, Phys. Rev. Lett. **94**, 072305 (2005).
[22] K. Huebner, F. Karsch, and C. Pica, Correlation functions of the energy-momentum tensor in SU(2) gauge theory at finite temperature, Phys. Rev. D **78**, 094501 (2008).
[23] H. B. Meyer, Transport properties of the quark-gluon plasma: A lattice QCD perspective, Eur. Phys. J. A **47**, 86 (2011).

[24] N. Astrakhantsev, V. Braguta, and A. Kotov, Temperature dependence of shear viscosity of $SU(3)$–gluodynamics within lattice simulation, J. High Energy Phys. 04 (2017) 101.

[25] L. D. Landau and E. M. Lifshitz, *Statistical Physics, Part 1*, 3rd ed. (Pergamon Press, Oxford, 1980).

[26] Y. Minami and Y. Hidaka, Relativistic hydrodynamics from the projection operator method, Phys. Rev. E **87**, 023007 (2013).

[27] M. Asakawa, T. Hatsuda, T. Iritani, E. Itou, M. Kitazawa, and H. Suzuki, Determination of reference scales for Wilson gauge action from Yang–Mills gradient flow, arXiv:1503.06516.

[28] R. V. Gavai, S. Gupta, and S. Mukherjee, The speed of sound and specific heat in the QCD plasma: Hydrodynamics, fluctuations and conformal symmetry, Phys. Rev. D **71**, 074013 (2005); Lattice quantum chromodynamics equation of state: A better differential method, Pramana **71**, 487 (2008).

[29] Y. Taniguchi, Energy-momentum tensor correlation function in $N_f = 2 + 1$ full QCD at finite temperature, arXiv:1711.02262.

[30] E. Itou and S. Aoki, QCD thermodynamics on the lattice from the gradient flow, *Proc. Sci.*, INPC2016 (2017) 342, [arXiv:1701.08983].